New Journal of Physics
The open-access journal for physics

Vortex synchronization in Bose–Einstein condensates: a time-dependent Gross–Pitaevskii equation approach

Ryan Barnett[1,2], **Edward Chen**[1] **and Gil Refael**[1]

[1] Department of Physics, California Insttute of Technology, MC 114-36, Pasadena, CA 91125, USA

[2] Joint Quantum Institute and Condensed Matter Theory Center, Department of Physics, University of Maryland, College Park, MD 20742, USA

E-mail: rbarnett@umd.edu

New Journal of Physics **12** (2010) 043004 (13pp)
Received 25 January 2010
Published 1 April 2010
Online at http://www.njp.org/
doi:10.1088/1367-2630/12/4/043004

Abstract. In this work, we consider vortex lattices in rotating Bose–Einstein condensates composed of two species of bosons having different masses. Previously (Barnett *et al* 2008 *New J. Phys.* **10** 043030), it was claimed that the vortices of the two species form bound pairs and the two vortex lattices lock. Remarkably, the two condensates and the external drive all rotate at different speeds owing to the disparity of the masses of the constituent bosons. In this paper, we study the system by solving the full two-component Gross–Pitaevskii equations numerically. Using this approach, we verify the stability of the putative locked state that is found to exist within a disc centered on the axis of rotation and that depends on the mass ratio of the two bosons. We also derive a refined estimate for the locking radius tailored to the experimentally relevant case of a harmonic trap and show that this agrees with the numerical results. Finally, we analyze in detail the rotation rates of the different components in the locked and unlocked regimes.

Contents

1. Introduction 2
2. Background 3
2.1. Two-component GPEs 3
2.2. Interspecies vortex attraction and locking 4
3. Results and discussion 6
4. Experimental considerations and concluding remarks 9
Acknowledgments 10
Appendix A. Density profile for a single vortex 10
Appendix B. Numerical methods 11
References 13

1. Introduction

One of the most striking manifestations of the quantum-mechanical nature of superfluids under rotation is the formation of quantized vortices [2, 3]. Perhaps the most natural arena to controllably investigate the physics of vortices is Bose–Einstein condensates (BECs) of alkali atoms [4–6]. For the simplest case where the condensate is composed of a single type of atom without spin degrees of freedom, a triangular lattice is formed [7, 8]. On the other hand, for multicomponent systems (composed of mixtures of atoms or spinor condensates, for instance), the order parameter has additional degrees of freedom, resulting in more complex vortex lattice structures (see, for example, [9–13]).

For the classic problem of an ideal fluid in a container rotating at rate $\mathbf{\Omega}$, the steady-state local velocity is $\mathbf{v} = \mathbf{\Omega} \times \mathbf{r}$, where $\mathbf{r}$ is the distance from the axis of rotation. Since this velocity has a nonvanishing curl everywhere ($|\nabla \times \mathbf{v}| = 2\Omega$), it is not a permissible flow for a superfluid that is supposed to be inherently irrotational ($\mathbf{v} = \frac{\hbar}{m}\nabla\theta$ with θ being the phase of the SF order parameter). However, superfluids are well known to mimic the classical rigid-body rotation *on average* by forming a vortex lattice where the density of these vortices is given by the Feynman relation [3, 8]

$$\rho_{\mathrm{v}} = \frac{m\Omega}{\pi\hbar}, \tag{1}$$

where m is the mass of the constituent bosons and Ω is the rate at which the superfluid is rotating, which is equal to the rotational rate of the walls of the container.

In a previous work [1], it was considered how the situation described above generalizes to the problem of two-component BECs composed of atoms having different masses. More specifically, equation (1) naturally generalizes, for two-component systems, to

$$\rho_{\mathrm{v}}^1 = \frac{m_1\Omega_1}{\pi\hbar}, \quad \rho_{\mathrm{v}}^2 = \frac{m_2\Omega_2}{\pi\hbar}, \tag{2}$$

where m_1 and m_2 are the masses of the bosons in the two constituent condensates and Ω_1 and Ω_2 are the angular rates at which the two superfluids are rotating. For the case where there is a negative interspecies scattering length, the attraction between species will lead to an

attractive interaction between vortices of the two species. When this interaction is sufficiently large, one has the situation where the vortices form bound pairs, forcing the densities of the two vortex lattices to be the same: $\rho_{\rm v}^1 \approx \rho_{\rm v}^2$. For this case, equations (2) imply that the two superfluids (taking without loss of generality $m_1 > m_2$) will rotate at different speeds $\Omega_1 < \Omega_2$. This counterintuitive state results from the quantum mechanical nature of the superfluid and has no analogue in the classical fluid case.

In [1], we argued for the possible existence of this state by making an ansatz for the short-ranged interspecies interaction and performed a two-body force calculation using it. This gave a quantitative prediction for the distance from the center of the condensate at which the vortex pairs become unbound, resulting from the growth of the Magnus force, which is referred to as the locking radius. In [1], we also provided numerical results obtained after studying this state by using the dual coordinate representation for the vortices (using a logarithmic interaction) and taking an ansatz for interspecies interaction. In the current paper, we study the system by using numerical integration of the full two-component Gross–Pitaevskii equation (GPE). The starting point here is more fundamental and makes no assumptions about the way vortices interact. We will verify that the locked states are stable for a range of parameters. Furthermore, we will see that the analytic prediction for the locking radius agrees well with the numerical results.

The paper is organized as follows. In section 2.1, we provide definitions and set the notation for the treatment of the GPE. In section 2.2, we summarize the derivation of the locking radius previously given in [1], which is based on a two-body force calculation. The main results of the paper are presented in section 3. Here, we provide the vortex lattice structures determined numerically and compare them with the estimate for the locking radius. Finally, in section 4, we provide a discussion of potential experiments for realizing this effect and then conclude.

2. Background

2.1. Two-component GPEs

Our analysis starts with the two-component Gross–Pitaevskii energy functional in the frame of reference rotating at angular rate Ω_d. This is given by $E = E_1 + E_2 + E_{12}$, where

$$E_1 = \int \mathrm{d}^2 r \left(\frac{\hbar^2}{2m_1} |\nabla \psi_1|^2 + V_1 n_1 + \frac{1}{2} g_1 n_1^2 - \Omega_d \psi_1^* L_z \psi_1 \right), \tag{3}$$

$$E_2 = \int \mathrm{d}^2 r \left(\frac{\hbar^2}{2m_2} |\nabla \psi_2|^2 + V_2 n_2 + \frac{1}{2} g_2 n_2^2 - \Omega_d \psi_2^* L_z \psi_2 \right), \tag{4}$$

and

$$E_{12} = g_{12} \int \mathrm{d}^2 r \; n_1(\mathbf{r}) n_2(\mathbf{r}). \tag{5}$$

In these equations, V_1 and V_2 are the confining potentials of the BECs, which we will assume to be harmonic. The intraspecies and interspecies scattering strengths are defined as $g_{1,2}$ and g_{12}, respectively. The angular momentum operator, as usual, is defined as $L_z = x p_y - y p_x$, where $p_{x,y} \equiv -\mathrm{i}\hbar \partial_{x,y}$.

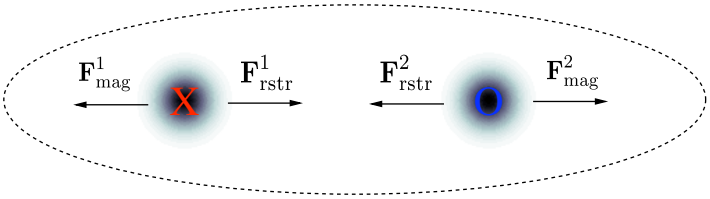

Figure 1. A bound pair of vortices occurring in the locked state composed of a mixture of BECs with $m_1 > m_2$. The vortex in the heavier species is denoted with an '$\times$', while that in the lighter species is denoted with an '$\circ$'. The center of the condensate is taken to be to the left of this bound pair. The attractive short-ranged interspecies force $\mathbf{F}^{1,2}_{\rm rstr}$ serves to bind the vortex pairs together. This is counterbalanced by the Magnus force $\mathbf{F}^{1,2}_{\rm mag}$, which increases from the center of the condensate. Note that the healing length of the superfluid is larger than the sphere representing vortices in this figure.

Varying this energy with respect to ψ_1 and ψ_2 and introducing the chemical potentials μ_1 and μ_2 to enforce particle number conservation gives the two-component GPEs

$$\mu_1\psi_1 = -\frac{\hbar^2}{2m_1}\nabla^2\psi_1 + V_1\psi_1 + g_1 n_1\psi_1 + g_{12}n_2\psi_1 - \Omega_d L_z\psi_1, \tag{6}$$

$$\mu_2\psi_2 = -\frac{\hbar^2}{2m_2}\nabla^2\psi_2 + V_2\psi_2 + g_2 n_2\psi_2 + g_{12}n_1\psi_2 - \Omega_d L_z\psi_2. \tag{7}$$

In appendix B, we describe how these coupled equations are solved numerically to find minima of the energy E.

2.2. Interspecies vortex attraction and locking

In this section, for completeness, we provide an estimate of the locking radius of the vortex-bound state based on a two-vortex calculation. This calculation is presented in more detail in [1]. We first consider the state for the case where the interspecies interaction is large and all of the vortices of one species are bound with that of the other due to the strong short-ranged attractive force. A bound pair of vortices is depicted in figure 1. The vortex binding causes the two superfluids to rotate at different rates (because of the different masses and the Feynman relation), creating a Magnus force that tries to rip the bound pair apart. The Magnus force is balanced by the short-ranged interspecies vortex interaction resulting from the overlap of the vortex cores. However, since the Magnus force grows linearly with distance from the center of the condensate, it will eventually overcome the short-ranged interspecies attraction. The point at which this occurs we refer to as the locking radius.

We will now put the previous arguments on a more quantitative footing. A vortex sitting at rest in a superfluid flowing at velocity $\mathbf{v}$ will experience a force perpendicular to the flow

$$\mathbf{F}_{\rm mag} = 2\pi\hbar n_0 \mathbf{v}\times\hat{\kappa}, \tag{8}$$

the so-called Magnus force [8], where $\hat{\kappa}$ is a unit vector centered at the vortex pointing out of the plane. Assuming that the system is composed of entirely locked vortex lattices, we

have, for the vortex densities, $\rho_v^{(1)} = \rho_v^{(2)}$. This, via the Feynman relations, gives

$$m_1\Omega_1 = m_2\Omega_2, \tag{9}$$

where Ω_1 and Ω_2 are the angular rotational rates of the two superfluids. Since $m_1 > m_2$ the superfluids will rotate at different rates, which will lead to the Magnus forces pulling the bound pair apart.

The short-ranged interspecies interaction arising from E_{12} defined in equation (5) will counteract the Magnus force. We refer to this as the 'restoring force'. In order to obtain an analytic expression for this interaction, we take a Gaussian ansatz for the density profile about a vortex. Specifically, for a vortex in species α centered at $\mathbf{r}_0$, we take

$$n_\alpha(\mathbf{r}) = n_0^\alpha(1 - \mathrm{e}^{-|\mathbf{r}-\mathbf{r}_0|^2/\lambda_\alpha^2}), \tag{10}$$

where λ_α is of the order of the superfluid coherence length [1]. We take

$$\lambda_\alpha = 1.781\xi_\alpha \tag{11}$$

for the value of this length parameter. This is a slight modification of the analysis in [1], where the simpler case of $\lambda_\alpha = \xi_\alpha$ was used. We choose the nonuniversal constant in equation (11) such that the ansatz in equation (10) provides a better fit to the density surrounding a vortex. For a detailed discussion of this, see appendix A.

Inserting this ansatz for two vortices separated by distance d into equation (5), we find

$$E_{12} = g_{12}n_0^1n_0^2\pi\frac{\xi_1^2\xi_2^2}{\lambda_1^2+\lambda_2^2}\mathrm{e}^{-d^2/(\lambda_1^2+\lambda_2^2)}, \tag{12}$$

where we have dropped terms that do not depend on the vortex separation. The interspecies force immediately follows from the derivative of this interaction energy and is

$$\mathbf{F}_{\mathrm{rstr}}^\alpha = -2\pi|g_{12}|n_0^1n_0^2\frac{\lambda_1^2\lambda_2^2}{(\lambda_1^2+\lambda_2^2)^2}\mathrm{e}^{-d^2/(\lambda_1^2+\lambda_2^2)}\mathbf{d}. \tag{13}$$

Balancing the forces on each vortex in the frame of reference rotating at the drive frequency, we have $F_{\mathrm{mag}}^1 = F_{\mathrm{rstr}}^1$ and $F_{\mathrm{mag}}^2 = F_{\mathrm{rstr}}^2$, as is illustrated in figure 1. Since the restoring force acting on either species has the same magnitude, we have that $F_{\mathrm{mag}}^1 = F_{\mathrm{mag}}^2$. The Magnus force on species α in the frame rotating with the vortex lattice at frequency Ω_{v} is given by

$$F_{\mathrm{mag}}^\alpha = 2\pi\hbar n_{\mathrm{o}}^\alpha|\Omega_\alpha - \Omega_{\mathrm{v}}|r, \tag{14}$$

which grows linearly with the distance from the center of the condensate r. Also, note that the restoring force will not depend on the position in the condensate. A bound vortex pair will become unstable when the Magnus force is equal to the maximum possible value of the restoring force. This works out to

$$\begin{aligned} r_c &= \sqrt{\frac{1}{2e}}\frac{|g_{12}|}{\hbar\Omega_v}\frac{m_1n_0^2+m_2n_0^1}{m_1-m_2}\frac{\lambda_1^2\lambda_2^2}{(\lambda_1^2+\lambda_2^2)^{3/2}} \\ &= 0.7638\,\frac{|g_{12}|}{\hbar\Omega_v}\frac{m_1n_0^2+m_2n_0^1}{m_1-m_2}\,\frac{\xi_1^2\xi_2^2}{(\xi_1^2+\xi_2^2)^{3/2}}. \end{aligned} \tag{15}$$

It also follows from this analysis that inside the locked region of the lattice, the superfluids will rotate with different angular velocities

$$\Omega_1 = \frac{(n_0^1 + n_0^2)m_2}{m_1 n_0^2 + m_2 n_0^1}\Omega_v < \Omega_v < \Omega_2 = \frac{(n_0^1 + n_0^2)m_1}{m_1 n_0^2 + m_2 n_0^1}\Omega_v. \tag{16}$$

A more detailed derivation of these expressions can be found in [1].

3. Results and discussion

We discuss below the results of the numerical simulation. Firstly, we provide the parameters that were used for the computations. For simplicity, we restrict our attention to the simplest case where $g_1 = g_2$, and we fix the interspecies scattering strength such that $|g_{12}|/g_1 = 2/3$. Furthermore, we take the number of particles in each species to be the same: $N_1 = N_2$. We set the dimensionless parameter defined as $\tilde{g} \equiv \frac{m}{\hbar^2} g_1 N_1$ to be $\tilde{g} = 2 \times 10^4$, which is in line with the values from typical experiments[3]. We take the two trapping potentials to be harmonic and adjust their curvatures ω_1 and ω_2 so that the density profiles of the two species have the same Thomas–Fermi profiles[4]. Finally, we rotate the system at 0.9 times the critical rate at which the condensate becomes unstable due to centrifugal forces. We discretize the system on a 200×200 grid, and propagate the system in imaginary time intervals of $\Delta\tau = 0.01\frac{1}{\hbar\omega_x}$.

We first consider the simplest case where the masses of the two species are the same. For this state, we take the initial wavefunction to be a perfect triangular lattice of vortices with density given by the Feynman relation, equation (1). This structure is then relaxed by evolving the wavefunctions in imaginary time using the methods described in appendix B. As expected, these vortex lattices remain fully locked. The relaxed structures show small deviations from the perfect triangular initial structure owing to the effects of the trap [14]. The density profiles of these are shown in figure 2 in panels (1a) and (1b). The positions of the vortices are determined by analyzing the phases of the relaxed wavefunctions. Using this relaxed structure as the initial state, we change the mass ratios and propagate the wavefunctions in imaginary time until convergence. Specifically, we consider the m_1/m_2 ratios of 1.2, 1.4. and 1.6, shown in figure 2.

To compare these numerical results to our estimate for the locking radius described in section 2.2, we need to tailor equation (15) to the case of a harmonic trap. We take the density profiles used in equation (15) to have the Thomas–Fermi form

$$n_{1,2} = n_0\left(1 - \left(\frac{r}{R_{TF}}\right)^2\right), \tag{17}$$

where n_0 is the density at the center of the trap and R_{TF} is the Thomas–Fermi radius (note that we are considering only the case where the two condensates have the same radius). Inserting this profile into equation (15) (taking the correct dependence of the coherence lengths on the

[3] Such a value would be obtained, for instance, for a condensate of 3×10^6 ^{87}Rb atoms with condensate thickness $d_z = 10\,\mu$m. This then gives $\tilde{g} = \frac{4\pi a}{d_z} N \approx 2 \times 10^4$, where we take $a = 106a_0$ for the s-wave scattering length.

[4] We choose the trapping potentials such that the density profiles are the same for simplicity. For the more general cases where the particle density and size of the clouds vary, the same physics of vortex locking will survive.

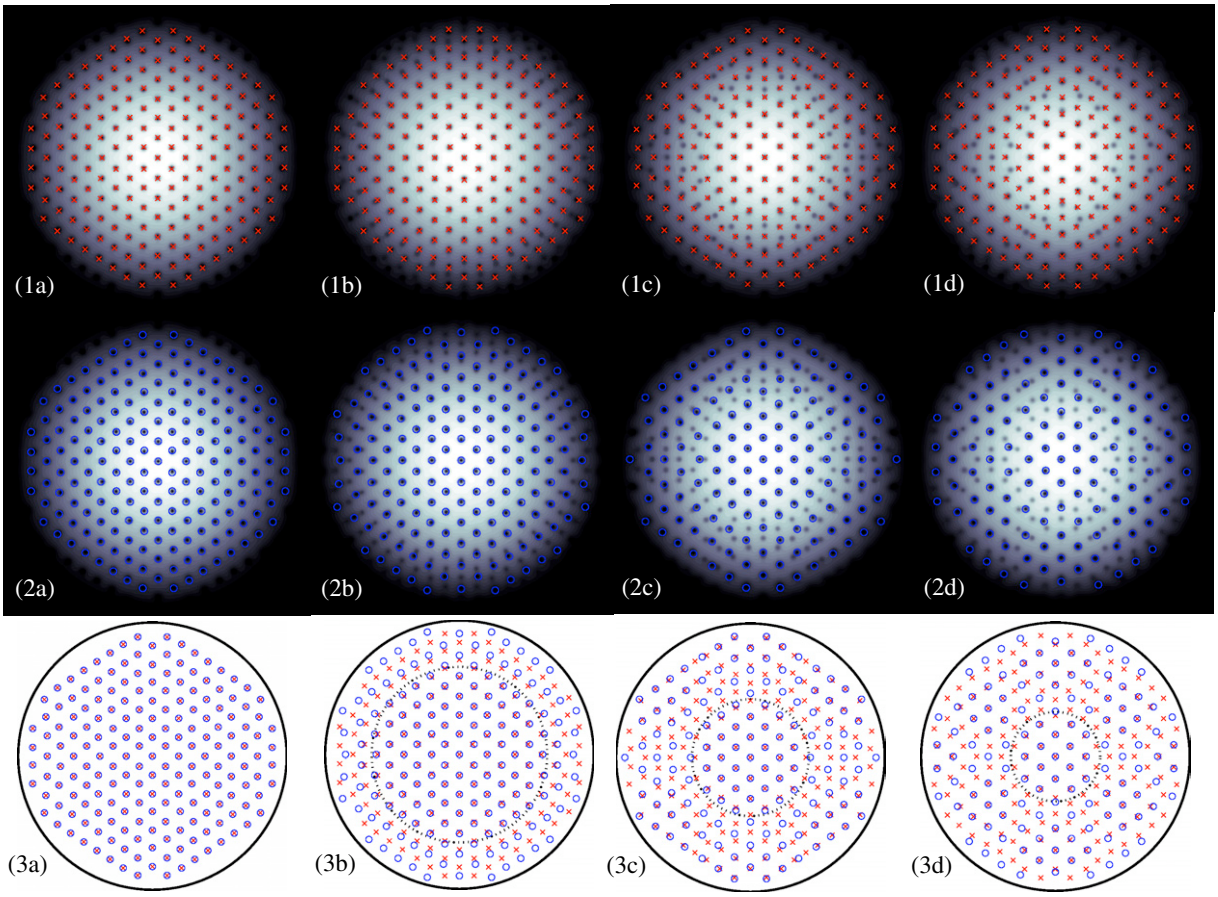

Figure 2. Relaxed vortex lattices for several mass ratios. Rows 1 and 2 are the density profiles of species 1 and 2, respectively, as a function of position. Superimposed over these images are the vortex positions marked with red ×s and black ○s. Row 3 gives the positions of both vortex species for comparison. In this row, the dotted circle is the estimate for the locking radius based on the two-body calculation showing good agreement with the numerics. Columns a, b, c and d are for the mass ratios of $m_1/m_2 = 1.0$, 1.2, 1.4 and 1.6, respectively.

density), one finds

$$r_{\rm c} = r_{\rm c}^0 \sqrt{1 - \left(\frac{r_{\rm c}}{R_{\rm TF}}\right)^2}, \tag{18}$$

where r_c^0 is equation (15) evaluated for parameters at the center of the trap. This equation can then be solved for $r_{\rm c}$ to obtain the renormalized value of the locking radius

$$r_{\rm c} = \frac{r_{\rm c}^0}{\sqrt{1 + \left(\frac{r_{\rm c}^0}{R_{\rm TF}}\right)^2}}. \tag{19}$$

This indicates that near the center of the condensate, we will have $r_{\rm c} \approx r_{\rm c}^0$ as expected. Also, the locking radius will never exceed the radius of the condensate as expected. The reduction of the

bare value of the locking radius can be qualitatively understood as follows. The Magnus force is proportional to the superfluid density, while the restoring force is proportional to this density squared. Therefore, near the edge of the condensate where the density is considerably smaller than its value at the center, the Magnus force will be favored, thereby suppressing the locking radius.

The third column of figure 2 shows the positions of the vortices of the two species, labeled as $\times$s and $\circ$s. The widths of these labels are roughly the size of the coherence length of the condensates. Superimposed on this is the locking radius predicted by equation (19) (using equation (19) for the bar locking radius) shown as a dotted line. This shows that the analytic results provide an excellent estimate of the locking radius. Note that due to the strong interactions between the two condensates, an unbound vortex in one species will create a local minimum in the other. Such features can be seen in columns c and d of figure 2. These local depletions should not be mistaken for vortices, which are defined by the phase behavior of the wavefunctions.

To obtain a more detailed understanding of the locking phenomena, it will be useful to look at the phase gradients of the wavefunctions in addition to the densities we were considering above. In fact, equation (16) makes a quantitative prediction for the angular velocities in the locked regime which can be directly tested by our numerics. Recalling that, for simplicity, we have chosen the trapping potential such that $n_0^1 = n_0^2$, equation (16) directly gives

$$\Omega_1 = \frac{2m_2}{m_1 + m_2}\Omega_d = \frac{m_2}{m_1}\Omega_2. \tag{20}$$

From our relaxed vortex structures, we can compute the rate at which each constituent superfluid is rotating. The average angular velocity of each component at distance r from the center of the condensate is given by $\Omega_1(r) = v_1(r)/r$ and $\Omega_2(r) = v_2(r)/r$, where v_1 and v_2 are the superfluid flow velocities averaged over a circle of radius r from the center of the condensate. More specifically, these are defined as

$$v_1 = \frac{1}{2\pi r}\oint \mathrm{d}\mathbf{r}\cdot\mathbf{v}_1, \qquad v_2 = \frac{1}{2\pi r}\oint \mathrm{d}\mathbf{r}\cdot\mathbf{v}_2. \tag{21}$$

Here $\mathbf{v}_1$ and $\mathbf{v}_2$ are, as usual, given by the gradient of the phase of the wavefunctions: $\mathbf{v}_1 = \frac{\hbar}{m_1}\nabla\theta_1$, $\mathbf{v}_2 = \frac{\hbar}{m_2}\nabla\theta_2$. In figure 3, we plot v_1, $\frac{2m_2}{m_1+m_2}v_d$ and $\frac{m_2}{m_1}v_2$, which directly provides a test for equation (20); all the quantities should be equal in the locked regime. We plot the above quantities for the two larger mass ratios $m_1/m_2 = 1.4$ and $m_1/m_2 = 1.6$ and note that the other mass ratios exhibit similar behavior. One sees that each of the three quantities shows good agreement in the locked regime. Note that due to the discreteness of the circulation of the vortices (each contributes a unit of $\frac{h}{m_1}$ or $\frac{h}{m_2}$ to equations (21)), the curves for v_1 and v_2 are nonmonotonic.

As we have shown, our theory provides a good description of the behavior inside the locked regime and the distance at which this state will become unstable. However, the general behavior for $r > r_c$ is a more complicated matter to address quantitatively. Qualitatively, as shown in figure 2, the vortices outside of the locking radius form triangular lattices. However, if vortices of two different species are nearby, the short-ranged attractive interaction given by E_{12} will serve to bind them together, locally distorting the triangular lattice to minimize the energy.

Finally, it is worth noting that interesting predictions of locked or 'vortex molecule' states were previously made in [15, 16]. These papers considered a rotating mixture of atoms in two different hyperfine states which are coupled through an external field. However, for this system

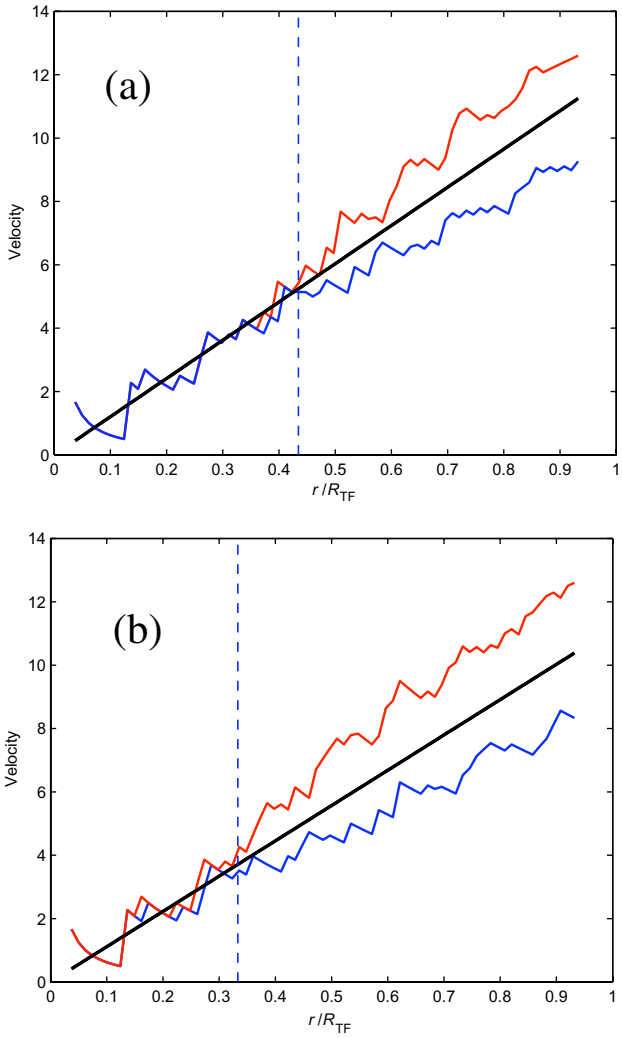

Figure 3. The quantities v_1 (red), $\frac{2m_2}{m_1+m_2}v_d$ (black) and $\frac{m_2}{m_1}v_2$ (blue) as a function of distance from the center of the condensate. v_1 and v_2 are the superfluid velocities of the two species averaged over a circle of radius r from the center of the condensate. v_d is determined through the rotation rate: $v_d = r\Omega_d$. The unit of velocity for these figures is $\sqrt{\hbar\omega_1/m_1}$. The vertical dashed lines indicate the locking radius determined from equation (19).

there is no intrinsic frustration for the vortex lattices since the masses of the two different bosonic species are the same. Therefore, none of the physics where the subsystems rotate at different rates will occur there.

4. Experimental considerations and concluding remarks

The main requirement for realizing the locked state is a BEC composed of a binary mixture of atoms having different masses and negative scattering length. Such a transition could be tuned with an interspecies Feshbach resonance, which has been found in Li–Na [17] and

Rb–K [18] mixtures. These mixtures have mass ratios of 3.3 and 2.2, respectively. Another promising experimental system is mixtures of two isotopes of a particular atom. For instance, the interspecies scattering lengths of different species of Yb have been analyzed in [19] and are often found to be negative. Since the mass ratios for different isotopes are closer to unity, it is not necessary to have a strong attractive interaction (often requiring a Feshbach resonance) to reach the vortex-locked state for this case.

Note that these results are closely related to the experiment described in [20]. Here a single-component BEC is stirred by a rotating optical lattice, which acts as vortex pinning sites. When the optical lattice is rotated at the speed for which the density of the pinning sites matches the density of the vortex lattice predicted by equation (1), a completely locked state is observed. Away from this resonance, a similar analysis as described above will predict a disc of bound vortices.

In conclusion, we report here our confirmation of the putative vortex-locked state that we proposed in [1]. For this state, the two superfluids and the stirring potential all rotate at different rates, exhibiting an unusual effect due to the quantum mechanical nature of superfluids. In the present paper, we show that such a state exists within a disc that is centered on the axis of rotation and has a size that agrees well with an analytical estimate. Note that our numerical analysis did not assume anything about the vortex–vortex attraction (unlike our theoretical analysis, which assumes equation (12) and evolves the GPEs directly). Our results (both analytical and numerical) rely on approaching this state from the fully locked state. Experimentally, this is probably most easily realized by controllably adjusting an interspecies Feshbach resonance. Alternatively, one can use an optical lattice to control the effective masses of the atoms by varying the lattice depth.

Acknowledgments

We thank M Porter and H-P Büchler for their collaboration in a related previous work. We also thank L Baksmaty for valuable advice on numerical methods. This work was supported by the Sherman Fairchild Foundation (RB); the Caltech SURF program (EC); and the Packard Foundation, the Sloan Foundation, the Institute for Quantum Information under NSF grants PHY-0456720 and PHY-0803371 and the Research Corporation Cottrell Scholars program (GR).

Appendix A. Density profile for a single vortex

In order to find the short-ranged interspecies vortex interaction, we need to know the behavior of the density of the condensate about a vortex. To this end, we consider the GPE for a single component BEC having a vortex at the origin. That is, we write $\psi = f\mathrm{e}^{i\theta}$ and take $\theta = \varphi$, where φ is the azimuthal angle from the polar coordinates. Substituting this into the GPE leads to the following equation dictating the density profile:

$$-\frac{\hbar^2}{2m}\frac{1}{r}\partial_r(r\partial_r f) + \frac{\hbar^2}{2m}\frac{f}{r^2} + gf^3 = \mu f. \tag{A.1}$$

The density $n = f^2$ resulting from the numerical solution of this equation is shown in figure A.1.

The numerical solution shows that the density behavior close to the vortex core ($r \ll \xi$) is $n(r) \approx 0.340\, n_0(\frac{r}{\xi})^2$. On the other hand, the long-distance behavior is found to be

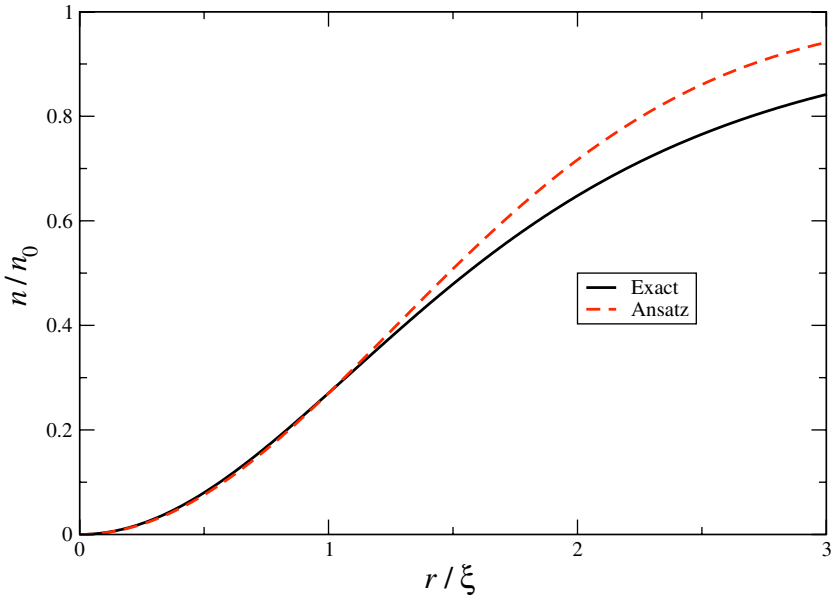

Figure A.1. Solid line: the density profile for a single vortex at $r = 0$ found by numerically solving equation (A.1). Dashed line: ansatz density profile $n(r) = n_0(1 - e^{-r^2/\lambda^2})$, where λ is selected so that the two densities agree at one coherence length away from the vortex center. The vertical lines give the locking radius.

$n(r) = n_0(1 - (\frac{\xi}{r})^2)$. To make our work amenable to analytic treatment, we take the following ansatz for the vortex profile:

$$n(r) = n_0(1 - e^{-r^2/\lambda^2}), \tag{A.2}$$

where λ is a parameter of the order of the coherence length. Note that while this ansatz has the correct form close to the vortex core, the long-distance behavior differs considerably. Fortunately, our problem of vortex locking is dominated by the short-distance behavior, and we choose λ such that the two densities (numerical and ansatz) agree at $r = \xi$, which requires $\lambda = 1.781\xi$, as shown in figure A.1.

Our positive results, confirming the vortex-locked state, also confirm our intuition that the origin of the phenomena is in the short-ranged attraction between vortices. As explained in [1] (but without proof), the algebraic decay of the superfluid order parameter of a single vortex does not imply that vortices of one species, when in a lattice, exhibit a power-law decaying force on the vortices on the other species. Unlike the single-species vortex–vortex force, which is the result of the inductive (kinetic) energy term in the GPEs, the interspecies force is a result of a density–density interaction. The density suppression due to a single vortex occurs since the superflow of the vortex effectively increases the mass terms V_1 and V_2 in equation (4). But in a lattice of vortices, the combined superflow vector is nearly zero (i.e. negligible compared to $\hbar/m_\alpha\xi_\alpha$) and, therefore, so is the respective density suppression.

Appendix B. Numerical methods

Since there are only rare occasions when the time-dependent GPE permits analytic solutions, numerical simulation is often the method of choice for theoretically studying BECs (for a recent

account of the numerical solution of the GPE, see [21]). In this section, for simplicity, we will only consider the single-component case, noting that the generalization to the two-component case is straightforward. To this end, the equation we wish to solve is

$$\hbar\frac{\partial\psi}{\partial\tau} = H\psi, \tag{B.1}$$

which describes the evolution of ψ in imaginary time, $\tau = \mathrm{i}t$. Under long enough evolution ψ will relax to the ground state of the Gross–Pitaevskii energy functional. In the above equation, H is given by

$$H = -\frac{\hbar^2}{2m}\nabla^2 + V_{\mathrm{trap}} + g|\psi|^2 - \Omega L_z. \tag{B.2}$$

We use a split-operator method to evolve the order parameter ψ as in equation (B.1). The idea behind the split-operator method is to approximate the evolution operator through imaginary time interval $\Delta\tau$, $U(\Delta\tau) = \mathrm{e}^{-H\Delta\tau}$, by a product of terms that are easily diagonalizable. Neglecting for the moment the rotational term in equation (B.2), H can be written as the sum of two terms, $H = T + V$, where $T = -\frac{\hbar^2}{2m}\nabla^2$ and $V = V_{\mathrm{trap}} + g|\psi|^2$. These terms are easily diagonalized in momentum and position space, respectively. The wavefunction ψ can then be advanced in time by $\Delta\tau$ by

$$\begin{aligned}\psi(\tau+\Delta\tau) &= \mathrm{e}^{-H\Delta\tau}\psi(\tau)\\ &\approx \mathrm{e}^{-(1/2)T\Delta\tau}\mathrm{e}^{-V\Delta\tau}\mathrm{e}^{-(1/2)T\Delta\tau}\psi(\tau),\end{aligned} \tag{B.3}$$

which is accurate to second order in $\Delta\tau$. The order parameter can then be evolved by taking successive Fourier (and inverse Fourier) transforms of ψ and multiplying by the factors $\mathrm{e}^{-(1/2)T\Delta\tau}$, $\mathrm{e}^{-V\Delta\tau}$ and $\mathrm{e}^{-T(1/2)\Delta\tau}$, respectively. Such Fourier transforms account for the bulk of the computational cost in this algorithm; thus, the use of the efficient fast Fourier transform algorithm is crucial.

A complication in the above occurs due to the nonlinearity of the GPE. That is, V in the above prescription for time evolution depends on the density $n = |\psi|^2$, and it is at first unclear for what time this quantity should be evaluated. It is shown in [22] that, provided we use the most updated version of the time-dependent density $n = |\psi|^2$, equation (B.3) will retain its second order accuracy. The final complication occurs from the rotational term in H, which is

$$R \equiv -\Omega L_z. \tag{B.4}$$

We have so far neglected this term since it is diagonalized in neither position nor momentum space and therefore cannot be included in either T or V. However, we note that R commutes with both T and V, so we can write

$$\begin{aligned}\psi(\tau+\Delta\tau) &= \mathrm{e}^{-H\Delta\tau}\psi(\tau)\\ &\approx \mathrm{e}^{-(1/2)T\Delta\tau}\mathrm{e}^{-R\Delta\tau}\mathrm{e}^{-V\Delta\tau}\mathrm{e}^{-(1/2)T\Delta\tau}\psi(\tau).\end{aligned} \tag{B.5}$$

Then we can perform a similar split-operator decomposition of the additional term as

$$\mathrm{e}^{-R\Delta\tau} \approx \mathrm{e}^{(1/2)\hbar\Omega x p_y\Delta\tau}\mathrm{e}^{-\hbar\Omega y p_x\Delta\tau}\mathrm{e}^{(1/2)\hbar\Omega x p_y\Delta\tau}. \tag{B.6}$$

Evolution of ψ by this factor can then be performed by taking the partial Fourier transform of ψ, that is, transforming over the x variables but leaving the y variables unchanged (and vice versa). This completes the overview of the numerical method used to solve the GPE. As stated earlier, the generalization to the two-component case is straightforward.

References

[1] Barnett R, Refael G, Porter M and Büchler H-P 2008 *New J. Phys.* **10** 043030
[2] Onsager L 1949 *Nuovo Cimento Suppl.* **6** 249
[3] Feynman R P 1955 Application of quantum mechanics to liquid helium *Progress in Low Temperature Physics* ed G J Gorter (Amsterdam: North Holland) p 17
[4] Matthews M R, Anderson B P, Haljan P C, Hall D S, Wieman C E and Cornell E A 1999 *Phys. Rev. Lett.* **83** 2498
[5] Madison K W, Chevy F, Wohlleben W and Dalibard J 2000 *Phys. Rev. Lett.* **84** 806
[6] Abo-Shaeer J R, Raman C, Vogels J M and Ketterle W 2001 *Science* **292** 476
[7] Tkachenko V 1966 *Sov. Phys.—JETP* **22** 1282
[8] Donnelly R J 1991 *Quantized Vortices in Liquid He II* (Cambridge: Cambridge University Press)
[9] Mueller E J and Ho T L 2002 *Phys. Rev. Lett.* **88** 180403
[10] Kasamatsu K, Tsubota M and Ueda M 2003 *Phys. Rev. Lett.* **91** 150406
[11] Mueller E J 2004 *Phys. Rev.* A **69** 033606
[12] Barnett R, Mukerjee S and Moore J E 2008 *Phys. Rev. Lett.* **100** 240405
[13] Cooper N R 2008 *Adv. Phys.* **57** 539
[14] Sheehy D E and Radzihovsky L 2004 *Phys. Rev.* A **70** 063620
[15] García-Ripoll J J, Pérez-García V M and Sols F 2002 *Phys. Rev.* A **66** 021602
[16] Kasamatsu K, Tsubota M and Ueda M 2004 *Phys. Rev. Lett.* **93** 250406
[17] Stan C A, Zwierlein M W, Schunck C H, Raupach S M F and Ketterle W 2004 *Phys. Rev. Lett.* **93** 143001
[18] Inouye S, Goldwin J, Olsen M L, Ticknor C, Bohn J L and Jin D S 2004 *Phys. Rev. Lett.* **93** 183201
[19] Kitagawa M, Enomoto K, Kasa K, Takahashi Y, Ciurylo R, Naidon P and Julienne P S 2008 *Phys. Rev.* A **77** 012719
[20] Tung S, Schweikhard V and Cornell E A 2006 *Phys. Rev. Lett.* **97** 240402
[21] Succi S, Toschi F and Vignolo P 2005 *Comput. Sci. Eng.* **7** 48
[22] Javanainen J and Ruostekoski J 2006 *J. Phys. A: Math. Gen.* **39** L179